

1 Candidate proteins associated with popping expansion

2 capacity of popcorn

3

4 Talita Mayara de Campos Jumes Gemelli^{1,a¶}, Isaac Romani^{1,b¶}, Natália Ferreira Dos
5 Santos^{1,a¶}, Maria de Fátima P.S. Machado³, Carlos Alberto Scapim², Gilberto Barbosa
6 Domont⁴, Fábio César Sousa Nogueira⁴, Adriana Gonela^{2*}

7

8 ¹Genetic Improvement Postgraduate Program - Department of Agronomy, State
9 University of Maringá, Maringá, Paraná, Brazil

10 ²Department of Agronomy, State University of Maringá, Maringá, Paraná, Brazil

11 ³Department of Biology, State University of Maringá, Maringá, Paraná, Brazil

12 ⁴Institute of Chemistry, Federal University of Rio de Janeiro, Rio de Janeiro, Brazil

13

14 #a Current address: Department of Agronomy, State University of Maringá, 87020-900,
15 Maringá, Paraná, Brazil

16 #b Current address: Ingá University Centre (Uningá), Maringá, Paraná, Brazil

17

18 *Corresponding author

19 E-mail: agonela@uem.br (AG)

20

21 ¶These authors contributed equally to this work.

22

23

24

25 **Abstract**

26 The mechanical resistance of the popcorn pericarp has a positive and direct relationship
27 to its expansion volume. It allows enough time for the endosperm to gelatinize completely
28 before its extravasation. Expansion is a polygenic trait that has been extensively studied.
29 However, no records in the literature indicate proteins that directly affect pericarp
30 thickness and integrity. Therefore, the present work aimed to identify candidate pericarp
31 proteins associated with the expansion capacity of popcorn kernels using the shotgun
32 proteomic approach. The analyses were carried out in the pericarp of two popcorn inbred
33 lines, P11 (expansion volume of 30 mL g^{-1}) and P16 (expansion volume of 14 mL g^{-1}), in
34 two developmental stages (15 and 25 DAP). A total of 803 non-redundant proteins were
35 identified. Most of them were involved in key processes associated with pericarp
36 development and thickening. Two candidate proteins stood out among the differentially
37 abundant proteins. Peroxidase was up-accumulated in P11/25 DAP (high popping
38 expansion) and was 1.498 times more abundant in this inbred line, while xyloglucan
39 endotransglucosylase/hydrolase was more abundant in P16 (low popping expansion) in
40 both developmental stages. Thus, the peroxidase protein increases expandability, whereas
41 xyloglucan endotransglucosylase/hydrolase decreases it, even though its specific role has
42 not been elucidated. These proteins should be further investigated, as they may be used
43 to improve expansion capacity in popcorn breeding programs.

44

45 **Introduction**

46

47 Popping is a physicochemical process in which the gelatinization and expansion
48 of starch occur simultaneously through the rupture of the pericarp when grains are

49 subjected to high temperatures (177-185 °C) for a short period [1, 2]. In this context,
50 popcorn maize [*Zea mays* L. var. *everta* (Sturtev) L. h. Bailey] is the species that presents
51 the best results to this process, as it has grains with morphological, physical-chemical,
52 and genetic characteristics that favor expansion [1, 3, 4, 5].

53 The pericarp of popcorn kernels performs one of the most important functions
54 during popping. It is more structurally organized in popcorn than in common corn [6],
55 maintaining the integrity of the kernel. Furthermore, it provides resistance to the increase
56 in internal pressure, reaching 760-930.8 kPa (or 10 atm). Finally, it increases heat-transfer
57 efficiency into the kernel for an ideal period until starch gelatinization occurs [1, 6, 7].
58 Pre-existing ruptures in the pericarp cell layers decrease the kernel resistance to the
59 pressure generated during heating, leading to internal steam escaping and producing
60 smaller or even no pieces of popped corn [6].

61 In the species *Zea mays*, the pericarp is formed by cells with a type II primary
62 cell wall, which stands out for having glucuronoarabinoxylan as the most abundant
63 hemicellulose (40-50%) linked to cellulose microfibrils. These components form a
64 complex network that confers rigidity and extensibility to the cell wall [8]. In turn,
65 xyloglucan appears in lower abundance (1-5%); therefore, it is a secondary component
66 [9]. However, even though it is less abundant, xyloglucan metabolism plays a more
67 central role in restructuring the cell wall of commelinoid monocots, such as maize [10].
68 One of the main enzymes that promote the cleavage and reassembly of xyloglucan
69 molecules is xyloglucan endotransglucosylase/hydrolase, which acts on β -1,4 or β -1,3
70 glycosidic bonds [11].

71 Lignin is the second most abundant component in pericarp cell walls, which
72 provides hydrophobicity and mechanical strength [12], in addition to protection against
73 biotic [13] and abiotic stresses [14]. Lignin results from the oxidative polymerization of

74 three canonical phenolic alcohols [sinapyl (S unit), coniferyl (G unit), and p-coumaryl (H
75 unit) alcohols] carried out by peroxidases and laccase enzymes in the secondary cell wall
76 [14-17]. Peroxidases have specialized activities according to the organ, cell, and
77 developmental stage. In conclusion, not only spatiotemporal regulation of gene
78 expression and protein distribution, but also differentiated oxidation properties of each
79 Prx define the function of this class of peroxidases [14].

80 Regarding the expansion capacity of popcorn, it is suggested that both lignin
81 content and composition contribute positively to the expansion volume [18]. However,
82 which genes/proteins are associated with lignin's highest content and composition has not
83 been determined. Thus, the present work aimed to identify candidate pericarp proteins
84 associated with the expansion capacity of popcorn kernels through shotgun proteomics
85 using iTRAQ® (Isobaric Tags for Relative and Absolute Quantitation - Sciex).

86

87 **Materials and methods**

88

89 **Popcorn inbred lines**

90

91 Two inbred lines of popcorn (early cycle) with different expansion volumes, P11
92 (expansion volume 30 mL g⁻¹) and P16 (expansion volume 14 mL g⁻¹), were used in the
93 quantitative proteome analysis.

94 The experiment was performed in the field (23°25'S, 51°57'W, 550 m altitude)
95 using the complete block design. Plots contained four 5-m long lines spaced 0.90 m apart
96 and plants spaced 0.20 m apart, with 10 repetitions. Irrigation was performed.

97 The plants were manually self-fertilized, and the ears were collected 15 and 25
98 days after pollination (DAP) (S1 Fig). Three ears of each treatment (lineages x

99 developmental stage x repetition) were collected, totaling four treatments: T1 (P11/15
100 DAP), T2 (P16/15 DAP), T3 (P11/25 DAP), and T4 (P16/25 DAP). First, the grains were
101 excised from the ears, and then the pericarps were removed, immediately frozen in liquid
102 nitrogen, and stored in an ultra-freezer (-80 °C) (S1 Fig 1).

103

104 **Extraction and preparation of protein samples**

105

106 After extracting proteins from the pericarp/aleurone [19], the samples were
107 lyophilized and stored in an ultra-freezer (-80 °C). The protein concentration was
108 obtained through the fluorimetric method using the Qubit® 2.0 Fluorometer (Invitrogen).
109 Afterward, the samples were diluted (1:10) in 200 mM TEAB (triethylammonium
110 bicarbonate) buffer, and they were reduced with 10 mM DTT (dithiothreitol) for 1 hour
111 at 25 °C. Subsequently, the samples were alkylated with 40 mM iodoacetamide (IAA) at
112 room temperature in the dark.

113 Proteins (50 µg) were digested with trypsin (Promega, Madison, WI, USA) at a
114 protein:trypsin ratio of 50:1. The samples were cleaned and purified using C-18 Macro
115 SpinColumns™ (Harvard Apparatus). Peptide samples were resuspended in 50 mM
116 TEAB buffer and quantified by the fluorimetric method using the Qubit® 2.0
117 Fluorometer. Subsequently, each treatment was divided into 25 µg aliquots of peptides.

118

119 **iTRAQ labeling and SCX (cation exchange fractionation)**

120

121 The peptides were processed according to the iTRAQ® 4-plex protocol. Peptides
122 from treatments T1 (P11/15 DAP), T2 (P16/15 DAP), T3 (P11/25 DAP), and T4 (P16/25

123 DAP) were labeled with reporter ions of 114, 115, 116, and 117 Da, respectively.

124 Biological triplicates (G1, G2, and G3) were performed per treatment.

125 Peptide samples tagged with iTRAQ® were resuspended in 100 µL of buffer A
126 [10 mM KH₂PO₄, 25% acetonitrile (ACN), pH 3] and loaded onto a cation exchange
127 Macro SpinColumn™ (Harvard Apparatus). The peptides were eluted at a gradient of
128 buffer A for 10 minutes at room temperature, with subsequent centrifugation at 100 rpm
129 for 3 minutes. This procedure was repeated twice, and the final eluate collected was
130 transferred to a new tube and identified as flow-through (FT).

131 The first fractionation was performed by adding 300 µL of buffer B (10 mM
132 KH₂PO₄, 25% ACN, 100 mM KCl) to the Macro SpinColumn. After centrifugation at
133 100 rpm for 3 minutes, the content was collected and stored in a new tube designated 100.
134 Then, two more fractionation processes were carried out using 250 mM and 500 mM KCl,
135 thus obtaining fractions of 250 and 500. Residual salts were removed from the cationic
136 process using C-18 Macro SpinColumns™ (Harvard Apparatus).

137

138 **LC–ESI–MS/MS analysis based on LTQ Orbitrap**

139

140 Peptide samples were solubilized in 0.1% formic acid and fractionated using a
141 nano-LC Easy 1000 system (Thermo Fisher) coupled to an Orbitrap-type mass
142 spectrometer (Q Exactive Plus, Thermo Scientific).

143 For each sample, 2 µg of peptides was applied to a trap column (200-µm inner
144 diameter and 2-cm length) packed in-house with Reprosil-Pur C18 5-µm resin (Dr.
145 Maisch®) (200 Å pores). The peptides were eluted in an analytical column (75-µm inner
146 diameter and 18-cm length) packed in-house with Reprosil-Gold C18 3-µm resin (Dr. Maisch®)
147 (300 Å pores). Peptide separation was performed using a gradient from 95% solvent A

148 (5% ACN and 0.1% formic acid) to 40% solvent B (95% ACN and 0.1% formic acid)
149 over 120 minutes.

150 The Orbitrap mass spectrometer was controlled by Xcalibur 2.2 software, which
151 was programmed to operate in automatic data-dependent (DDA) mode. The mass
152 spectrum was acquired with a resolution of 70,000 to 200 m/z (mass/charge). The reading
153 spectrum comprised peptides with 375 to 2000 m/z.

154 The 15 most intense ions were fragmented and then subjected to MS/MS
155 acquisition using higher energy collision-induced dissociation (HCD). Each DDA
156 consisted of a scan survey comprising a range of 200-2000 m/z. Peptides with
157 undetermined charges and +1 were rejected. A 5% ammonia solution contained in a 15
158 mL tube with the lid open was placed close to the nESI region to avoid the effect of
159 increasing ionic charge caused by the iTRAQ 4-plex [20, 21].

160 The experiment consisted of a total of 36 mass spectrometer runs, with samples
161 derived from pericarp/aleurone, biological triplicates (G1, G2, and G3), four fractionation
162 steps (100, 250, 500, and FT), and technical triplicates (runs in the mass spectrometer).
163 All biological replicates and their respective fractionations were analyzed together.

164

165 **Data analysis**

166

167 Raw files were visualized using Xcalibur v.2.1 software (Thermo Scientific), and
168 data were processed using Proteome Discoverer v.1.4 software. *Zea mays* L. cv. B73 was
169 obtained from the UniProt Consortium (<http://www.uniprot.org/>) (UniProt, 2019), which
170 had 85,525 entries (downloaded in April 2016). Analyses were performed according to
171 the following parameters: 10 ppm tolerance for precursor ion masses, MS accuracy of 0.1
172 Da for HCD, two missed cleavages allowed for fully tryptic peptides,

173 carbamidomethylation of cysteine as a fixed modification, oxidation of methionine and
174 lysine and N-terminal oxidation caused by iTRAQ® as variable modifications.

175 Protein number and groups, peptide number, and the quantitative values of each
176 marker were estimated using the Proteome Discovery software through the SEQUEST
177 algorithm. The false discovery rate (FDR) was set at 1% for the detection of peptides and
178 proteins. The proteins received the UniProt Consortium identification codes.

179 PatternLab for Proteomics software (<http://www.patternlabforproteomics.org/>)
180 [22] was also used to identify the peptides and proteins. Briefly, the search was performed
181 with the Comet search tool limited to fully tryptic candidate peptides, while cysteine
182 carbamidomethylation and iTRAQ-4 (N-terminal and K) were defined as fixed
183 modifications. A cut-off point of 1% was established for FDR at the peptide level based
184 on the number of labeled decoys. This procedure was performed independently for each
185 data subset, resulting in an FDR value independent of the tryptic or charge state. In
186 addition, a peptide with a minimum length of six amino acids was required.

187 The results were post-processed to accept only PSMs with less than 6 ppm of the
188 global identification average. One-hit wonders (proteins identified with only one mass
189 spectrum) were considered only if the XCorr values were greater than 2.5. These criteria
190 led the values of FDRs (at the protein level) to be less than 1% for all the results surveyed.

191

192 Quantitative analysis of total proteins

193

194 The quantitative analysis for protein expression was conducted with PatternLab
195 for Proteomics software using the Isobaric Analyzer module [22]. In this module, iTRAQ
196 reporter ion intensities were extracted, applied to purity correction (as indicated in the
197 manufacturer's instructions), and then normalized by the signal from each isobaric marker

198 according to the total ion current for that respective reporter ion mass. PatternLab
199 provides features in its platform. Thus, we were able to perform a comparative data
200 investigation based on ratios provided by the two experimental conditions.

201 In this study, analyses were performed based on the treatment ratios, with the
202 results for lines P11 and P16 established in the numerator and denominator, respectively,
203 for the two developmental stages (15 and 25 DAP). Thus, the ratios analyzed were RI
204 ($P11_{15DAP}/P16_{15DAP}$) and RII ($P11_{25DAP}/P16_{25DAP}$).

205 The Isobaric Analyzer module employs a peptide-centric approach that assigns a
206 paired t-test with p-values to each peptide and then converges to a final p-value (at the
207 protein level) through Stouffer's method. To conduct statistical analysis, we assumed
208 log2-values of the integration value of the precursor (ICPL) or the reporter ion (iTRAQ)
209 and normalized them on sets of three replicates. An overall average with all values and
210 stages was estimated. By that, the samples became comparable by subtracting this
211 average. Finally, we merged the values of all replicates (considering each developmental
212 stage individually), and the total average was used to normalize each replicate. A protein's
213 log fold change was estimated by averaging the corresponding peptide log folds. Our
214 differential proteomic comparison considered only proteins identified with unique
215 peptides (i.e., peptides that map to a single sequence in the database), a paired t-test \leq
216 0.05, and an absolute peptide fold change cut-off higher or less than 1.5x.

217

218 **Bioinformatics analysis**

219

220 The proteins identified in the UniProt Consortium also received the official
221 nomenclature for the species *Zea mays* available in MaizeGDB (Maize Genetics and
222 Genomics Database) (<https://www.maizegdb.org/>).

223 The Search & Color pathways feature of KEGG Mapper (Kyoto Encyclopedia of
224 Genes and Genomes) (https://www.genome.jp/kegg/mapper/convert_id.html) [23]
225 together with MaizeMine v. 1.3 from MaizeGDB
226 (<http://maizemine.rnet.missouri.edu:8080/maizemine/templates.do>) [24] were used to
227 identify metabolic pathways. In addition, the proteins were subjected to functional
228 categorization of Gene Ontology (GO) terms for biological processes with the aid of the
229 Analysis Toolkit and Database for Agricultural Community program (AgriGO)
230 (<http://bioinfo.cau.edu.cn/agriGO/>) version 2.0 [24]. The statistical parameters used in
231 AgriGO were Fisher's exact test and the multi-test adjustment method of Yekutieli (FDR
232 under dependency) with a 5% significance level.

233

234 **Results**

235

236 **Identified proteins**

237

238 The protein and one-dimensional profiles obtained from the pericarp samples of
239 the two popcorn lines (P11 and P16) in the four analyzed treatments, T1 (P11/15 DAP),
240 T2 (P16/15 DAP), T3 (P11/25 DAP), and T4 (P16/25 DAP), showed a great abundance
241 of proteins between 20-97 kDa, in addition to good reproducibility of the profiles (S2
242 Fig.).

243 The quantitative characterization of the proteome based on iTRAQ® identified
244 3,924 proteins that assumed an FDR of 1% in the samples of the two popcorn lines, thus
245 determining high confidence in their identification. Of these, 803 were non-redundant and
246 were analyzed in more detail (S1 Table). The 803 proteins were categorized into nine

247 major biological processes (GO:0008150), eight molecular functions (GO:0003674), and
248 seven cellular components (GO:0005575) (Fig 1, S2 Table).

249

250 **Fig 1. Main GO terms related to Biological Processes, Molecular Function, and**
251 **Cellular Component of non-redundant proteins identified in the pericarp of popcorn**
252 **inbred lines P11 and P16.**

253

254 The categories that stood out the most in biological processes were metabolic (235
255 proteins) and cellular processes (159 proteins). Within the cellular processes, five proteins
256 (Q94KT7, expansin; B8A2X5 and B6SSX0, pectinesterase; B6SY11,
257 glycosyltransferase; B4F9X6, pectin acetylesterase, and A0A1D6MMX0,
258 glycosyltransferase family 61 protein) were identified in the plant-type cell wall
259 organization (GO:0009664); three proteins (B4FB81, fasciclin-like arabinogalactan
260 protein 6; B6SSV3, fasciclin-like arabinogalactan protein 7, and A0A1D6I6L8, fasciclin-
261 like arabinogalactan protein 8) were identified in plant-type secondary cell wall
262 biogenesis (GO:0009834); two proteins (B4FQS9, trans-cinnamate 4-monoxygenase
263 and B6U7D8, cinnamyl alcohol dehydrogenase) were linked to the lignin metabolic
264 process (GO:0009808), and one protein (B4FHS5, xyloglucan
265 endotransglucosylase/hydrolase) acted in the xyloglucan biosynthetic process
266 (GO:0010411), as well as in cell wall biogenesis (GO:0042546) and organization
267 (GO:0071555).

268 In the molecular function category, proteins were mainly allocated to catalytic
269 activity (266 proteins) and binding (199 proteins). In addition, another category that
270 deserves to be highlighted is antioxidant activity, in which nine proteins were assigned.
271 All these proteins are peroxidases (A0A1D6E530, B4FB95, B4FH35, B4FNL8, B4FU88,

272 B4FUT1, B6SI04, B6T6D4, and B6TWB1) with heme-binding activity (GO:0020037),
273 metal ion binding (GO:0046872), and peroxidase activity (GO:0004601). Additionally,
274 they are associated with response to stimulus.

275

276 **Differentially abundant proteins**

277

278 Thirty-nine differentially abundant proteins were identified in the
279 pericarp/aleurone of the two popcorn lines (Fig 2A, S3 Table). Early in development (15
280 DAP), eight differentially abundant proteins were identified (Fig 2A). Two proteins were
281 up-accumulated exclusively in the inbred line P16 (low expansion capacity), K7UBG7
282 (cullin-associated NEDD8-dissociated protein 1) and B6T6D4 (peroxidase) (Figs 2A and
283 2B). These proteins were allocated to genetic information processing and
284 phenylpropanoid biosynthesis pathways, respectively (Fig 3, S4 Table). Notably, the
285 peroxidase B6T6D4 was 0.565 times more abundant in P16 (15 DAP) than in P11 (Table
286 1). In addition, three up-accumulated proteins were identified in P11 (high expansion
287 capacity) at 15 DAP (Fig 2A). Two proteins, B6TI56 (ribose-5-phosphate isomerase) and
288 B6ST80 (auxin-repressed 12.5 kDa protein), were up-accumulated exclusively at this
289 developmental stage (Figs 2A and 2B), acting on the pentose phosphate and metabolic
290 pathways, respectively (Fig 3, S4 Table).

291

292 **Fig 2. Differentially abundant proteins identified in two popcorn inbred lines (P11**
293 **and P16) in two developmental stages (15 and 25 DAP) (A); relationship of up-**
294 **accumulated proteins in P16/15 DAP, P16/25 DAP, P11/15 DAP, and P11/25 DAP**
295 **(B).**

296

297 **Fig 3. Metabolic pathways of differentially abundant proteins identified in the**
298 **pericarp of two popcorn inbred lines (P11 and P16) in two developmental stages (15**
299 **and 25 DAP).**

300

301 At 25 DAP, among the 31 differentially abundant proteins identified, 18 were up-
302 accumulated exclusively in P16 (low expansion capacity), and 13 were only upregulated
303 in P11 (high expansion capacity) (Figs 2A and 2B, S3 Table). The vast majority of
304 proteins, both in the P16 (13 proteins) and P11 (11 proteins) inbred lines, were identified
305 in the global and overview map pathways (Fig 3). However, the up-accumulated proteins
306 B4FZU9 (dihydropyrimidine dehydrogenase NADP⁺ chloroplastic), B4FSX7 (-+
307 neomenthol dehydrogenase), and B7ZZM7 (eukaryotic translation initiation factor 2
308 subunit alpha) were exclusively detected in P16. These proteins are related to the
309 metabolism of other amino acids and metabolism of cofactors and vitamins, metabolism
310 of terpenoids and polyketides, translation and folding, and sorting and degradation
311 pathways. In turn, in P11 at 25 DAP, two proteins stood out, A0A1D6E530 (peroxidase)
312 and B4FUH2 (aspartate aminotransferase), which were identified in the phenylpropanoid
313 biosynthesis and amino acid metabolism pathways, respectively (Fig 3, S4 Table).
314 Peroxidase was 1.498 times more abundant in P11 than in P16 at 25 DAP (Table 1).

315 In addition, xyloglucan endotransglucosylase/hydrolase (B4FHS5) stood out. This
316 protein was up-accumulated exclusively in the inbred line P16 in the two stages of
317 pericarp development (Fig 2B, S3 Table), and it was identified in the metabolism pathway
318 (Fig 3, S4 Table). This protein was 0.414 and 0.469 times more abundant in the low
319 expansion capacity line than in the high expansion capacity inbred line at 15 and 25 DAP,
320 respectively (Table 1).

321

322 **Table 1. Up-accumulated proteins identified in lignin and hemicellulose metabolic**
323 **pathways.**

(Prot ID) Description	Log_e (x) of ratios*		p- value
	RI	RII	
(B4FHS5) Xyloglucan endotransglucosylase/hydrolase	-0.881		0.010
		-0.756	0.010
(B6T6D4) Peroxidase		-0.565	0.045
(A0A1D6E530) Peroxidase		0.404	0.010

324 *Note: RI, 15 DAP (P11/P16); RII, 25 DAP (P11/P16).

325

326 **Discussion**

327

328 The popcorn pericarp is directly related to the expansion capacity. It has a
329 mechanical resistance that allows it to withstand an internal pressure that can reach 930.8
330 kPa [1,6], thus allowing sufficient time for the endosperm to gelatinize completely before
331 its rupture.

332 The pericarp thickness is directly associated with its mechanical resistance. Some
333 studies have evaluated pericarp thickness [25,26], its type of inheritance [27] and integrity
334 [7], and the role the cellulose matrix plays in the retention of moisture inside the seed [28]
335 to correlate these traits with expandability. However, no work has sought to analyze the
336 pericarp proteome to identify proteins associated with expansion capacity.

337 In the present work, most of the proteins identified in the pericarp proteome of
338 seeds from two popcorn inbred lines (P11 and P16) in two developmental stages (15 and
339 25 DAP) were intrinsically involved in the key processes associated with pericarp
340 development and thickening (Fig 1, S1 Table). Metabolic process was the category that
341 presented the highest number of associated proteins (29.3%), emphasizing the primary

342 metabolic process with 66% of this total. The molecular functions of catalytic activity
343 and binding had 33% and 25%, respectively. For cellular components, the categories of
344 cell (13.8%) and cell part (13.8%) were the ones with the highest number of associated
345 proteins. These results are very similar to those obtained from the pericarp of the N04
346 popcorn inbred line evaluated in three stages of seed development (10, 20, and 33 DAP)
347 [29]. The only difference observed was an inversion between the molecular functions
348 binding and catalytic activity, with 45.87% and 41.46% of associated proteins,
349 respectively [29].

350 Ten proteins that regulate the organization of cell walls aiding in assembly,
351 arrangement of constituent parts, or disassembly of cell walls were identified (Fig 1).
352 Among them, expansin (Q94KT7) promotes the loosening and extension of cell walls,
353 interrupting the non-covalent bond between cellulose microfibrils and matrix glucans
354 [30,31]. Furthermore, this protein appears to be strongly bound to xylans present in type
355 II primary cell walls found in grasses such as popcorn maize [31].

356 The identification of proteins that regulate the organization of cell walls is
357 explained by the processes involved in pericarp development. The pericarp is a maternal
358 tissue originating from the ovary walls. After undergoing a period of cellular expansion
359 in the first 9 DAP, it collapses between 10 and 18 DAP. This phenomenon occurs after
360 partial resorption of cells to form the inner and outer pericarp, adjusting to the expanding
361 endosperm [32]. The 15 DAP time point analyzed in the present work comprises this
362 period of cellular collapse and reorganization.

363 Further in the development process, at approximately 20 DAP, the cells of the
364 inner pericarp collapse, while those of the outer pericarp elongate, causing a significant
365 thickening of the cell walls. Consequently, the pericarp thickens [32], forming a strong
366 protective layer. This thickening continues gradually until the later stages of maturation

367 [25]. The 25 DAP time point evaluated in the present study is included in this thickening
368 phase. Therefore, pericarp reorganization, expansion, and thickening processes, which
369 occur between 10 and 20 DAP, directly affect the number of identified proteins and the
370 complexity of observed biological and biochemical processes. Pericarp thickness is a
371 complex trait that has high heritability in the narrow sense (55-82%), involving additive,
372 dominant, and epistatic effects [27, 33], with QTLs and candidate genes associated with
373 it [24, 35].

374

375 **Differentially abundant proteins**

376

377 The protein profile, especially the differentially abundant ones, contributed
378 greatly to understanding the gene regulation during kernel pericarp development in the
379 two inbred lines of popcorn analyzed. It was possible to observe that the lines showed
380 regulation differences even at the same point in the plant cycle.

381 The highest number of up-accumulated proteins was identified in the inbred line
382 P16 (low expansion capacity), 83% at 25 DAP, all allocated to global metabolic pathways
383 (Fig 2, S3 Table). The remaining proteins were associated with secondary metabolism.
384 The same behavior was observed in the inbred line with high expansion capacity (P11);
385 77% of the proteins were allocated to global metabolic pathways.

386 The number of up-accumulated proteins identified in the two popcorn inbred lines
387 and their metabolic pathways was lower and different from what was observed in the
388 pericarp of N04 [29]. This difference is probably due to genotype, method of analysis,
389 and developmental stages. The authors pointed out that the number of proteins identified
390 varies according to the stage of development evaluated.

391

392 **Candidate proteins**

393

394 Three differentially abundant proteins stood out in the two popcorn inbred lines,
395 two in P16 (low expandability) and one in P11 (high expandability). Two are peroxidases,
396 and one is a xyloglucan endotransglucosylase/hydrolase (XTH). Peroxidases participate
397 in phenylpropanoid biosynthesis, specifically in lignin biosynthesis, and xyloglucan
398 endotransglucosylase/hydrolase is an enzyme that promotes the cleavage and reassembly
399 of xyloglucan molecules [31].

400

401 **Peroxidases**

402

403 The final step of lignin biosynthesis is the polymerization of monolignols (sinapyl
404 alcohol, S unit; coniferyl alcohol, G unit; and β -coumaryl alcohol, H unit) in the
405 secondary cell wall domains by peroxidases and laccases [14-17]. The function of these
406 enzymes is conditioned by spatio-temporal regulation of gene expression, as well as their
407 differentiated oxidation [14]. In this study, the peroxidases B6T6D4 and A0A1D6E530
408 were up-accumulated in P16/15 DAP and P11/25 DAP, respectively.

409 As previously mentioned, 25 DAP is the developmental stage in which the
410 secondary cell wall of the pericarp thickens, making it more rigid, that is, more lignified.
411 Therefore, the greater accumulation of the peroxidase A0A1D6E530 in the pericarp of
412 P11 makes its cell walls more rigid. Thus, it indicates why the pericarp of this inbred line
413 resists longer to increased pressure inside the kernel during the popping process [6, 7].
414 The content and composition of lignin present in the pericarp of three popcorn inbred
415 lines, including the two analyzed in the present work, have been evaluated [18].
416 According to the authors, there was a statistically significant difference (5% probability

417 by the F test) between the lignin content present in the pericarp of the popcorn inbred
418 lines. The lines with higher expansion volume values, including P11, presented higher
419 lignin contents, concluding that lignin positively contributes to the expansion volume
420 [18].

421 The gene that encodes the peroxidase A0A1D6E530 is *Zm00001eb076190*, also
422 called *Sb03g046810_2*, located on chromosome 2 (26,292,971-26,294,428) and available
423 in the Gramene database (<https://www.gramene.org/>). This gene was shown to be up-
424 regulated during 25 DAP in the highly expandable line P11.

425 P16 (low expansion capacity) presented increased peroxidase (B6T6D4)
426 accumulation at 15 DAP. This stage is inserted in the period of cellular collapse and
427 formation of the internal and external pericarp, with an adjustment for endosperm
428 expansion [32]. Class III peroxidases, where A0A1D6E530 and B6T6D4 belong, present
429 spatio-temporal regulation of gene expression, as well as differentiated oxidation
430 properties [14]. Therefore, the regulation of peroxidase B6T6D4 in P16 was probably
431 directed at the initial events of pericarp collapse and reorganization. Between 15 and 18
432 DAP, the pericarp reaches its maximum thickness in the seed basal region [36], thus
433 indicating that the peroxidase B6T6D4 from P16 is involved in pericarp thickening. In
434 contrast, the peroxidase A0A1D6E530 is linked to lignin deposition, making the pericarp
435 of P11 (high expansion capacity) more resistant.

436 Comparing the results obtained in the present work with those available in the
437 literature, especially with the 11 MetaQTLs associated with increased popcorn expansion
438 volume [35], it can be seen that the gene *Zm00001eb076190* that encodes a peroxidase
439 (A0A1D6E530) had not yet been reported. Therefore, this gene is an important addition
440 to understanding the studied trait and can be used for introgression in breeding programs
441 aiming to improve popcorn expansion capacity.

442

443 **Xyloglucan endotransglucosylase/hydrolase**

444

445 In P16 (low expansion capacity), at both 15 and 25 DAP, xyloglucan
446 endotransglucosylase/hydrolase (XTH) was up-accumulated. This protein is a member of
447 the GH16 (glycosidic hydrolase) family, actively acting to break β -1,4 or β -1,3 glycosidic
448 bonds in various CAZyme glucans and galactans (Carbohydrate-Active Enzymes
449 Database) [11, 37]. This enzyme exhibits transglycosylase (XET) and glycosidic
450 hydrolase (XEH) activity [31]. Like expansins, xyloglucan
451 endotransglucosylase/hydrolase is versatile in the metabolic process of cell wall
452 biogenesis and organization [31, 38-40]. When XET acts on xyloglucan, it provides a
453 reversible cell wall loosening mechanism necessary for plant cell expansion [41], while
454 XEH causes irreversible extension [11]. In addition, transglycolysation predominates
455 over hydrolysis unless the receptor concentration is very low [42].

456 Some XTH gene families have already been identified. For instance,

457 *Arabidopsis thaliana* presents 33 [43] genes while tomato (*Solanum lycopersicum* L.) has
458 25 members [44]. In monocots, such as wheat [45] and rice [46], 57 and 29 genes were
459 identified, respectively. In maize, the number of genes belonging to the XTH family is
460 unknown. However, *Zm1005* was identified [47]. This gene was validated on March 6,
461 2019, and published in the National Center for Biotechnology Information, receiving the
462 symbol *LOC542059* (or *xth1* and *GRMZM2G119783*), locus
463 tag *ZEAMMB73_Zm00001d024386*, located on chromosome 10, and containing 1,475
464 nucleotides (68,324,472 to 68,325,946) [48].

465 The expression of XTH family genes is normally tissue-specific and
466 developmental stage-dependent, as observed in *Oryza sativa* [43], *Triticum durum* [49],
467 and *Hordeum vulgare* [40]. XTHs act on xyloglucan, which is not the main hemicellulose

468 that contributes to cell wall organization in *Z. mays*. Nevertheless, it is suggested that
469 even though it is less abundant, xyloglucan metabolism plays a central role in
470 restructuring the cell wall of commelinoid monocots, such as maize [10]. In addition,
471 hydrolases also play a role in cell extension [31].

472 Considering the above, it would be possible to hypothesize that xyloglucan
473 endotransglucosylase/hydrolase (B4FHS5) affects the pericarp cell walls of P16 (low
474 expansion capacity) since this protein was up-accumulated in both developmental stages,
475 indicating that the *GRMZM2G119783* gene was up-regulated. In this context, it is
476 suggested that xyloglucan endotransglucosylase/hydrolase participates in regulating the
477 metabolic process of biogenesis and cell wall organization together with expansins,
478 promoting the irreversible loosening of the pericarp cell walls of P16 (low expansion
479 capacity). Thus, it makes it thinner and compromises its integrity, making it unable to
480 withstand the pressure generated inside the kernel. In this way, the pericarp is ruptured
481 before the endosperm is completely gelatinized, causing P16 to have a lower expansion
482 capacity. However, this hypothesis needs to be further investigated.

483

484 Conclusion

485

486 Our data strongly suggest that the peroxidase A0A1D6E530 increases the
487 expansion capacity of popcorn kernels by increasing the lignin content. On the other hand,
488 the xyloglucan endotransglucosylase/hydrolase B4FHS5 has been shown to play an
489 important role, yet to be elucidated, in the decrease of expandability. Since expansion
490 capacity is a polygenic trait, these two proteins and their respective genes stand out as
491 important candidates in this pathway, contributing positively and negatively to the

492 popping process, respectively. This information is unprecedented and can be used by
493 popcorn breeding programs.

494

495 Supporting information

496

497 **S1 Fig.** Seeds of inbred lines P16 (expansion volume 14 mL g⁻¹) and P11 (expansion
498 volume 30 mL g⁻¹) in both developmental stages.

499 (TIFF)

500 **S2 Fig.** Processing of seeds for further protein extraction. a) Ear of inbred line P11 (15
501 DAP); b) removal of individual seeds from the ear with a scalpel; c) longitudinal cut
502 performed in the kernel pericarp; d) pericarps separated from the seeds and frozen.

503 (TIFF)

504 **S3 Fig.** Protein profiles obtained in the pericarp of popcorn seeds of lines P11 and P16 in
505 the four treatments analyzed, namely, T1 (P11/15 DAP), T2 (P16/15 DAP), T3 (P11/25
506 DAP), and T4 (P16/25 DAP).

507 (TIFF)

508 **S1 Table.** Specific proteins identified in the pericarp of inbred lines P11 and P16.
509 (XLSX)

510 **S2 Table.** GO terms referring to biological processes (P), molecular function (F), and
511 cellular components (C) for pericarp proteins.

512 (XLSX)

513 **S3 Table.** Differentially abundant proteins identified in the pericarp of P11 and P16
514 inbred lines, considering the RI (P11_{15DAP}/P16_{15DAP}) and RII (P11_{25DAP}/P16_{25DAP}) ratios.
515 (XLSX)

516 **S4 Table.** Metabolic pathways that showed up-accumulated proteins in the pericarp of
517 popcorn inbred lines P11 and P16 during seed development at 15 DAP (ratio RI) and 25
518 DAP (ratio RII).

519 (XLSX)

520

521 **Acknowledgments**

522

523 The authors would like to thank the Coordination for the Improvement of Higher
524 Education Personnel (Coordenação de Aperfeiçoamento de Pessoal de Nível Superior –
525 CAPES), Prof. Carlos Alberto Scapim for providing the seeds of the popcorn maize lines,
526 and the Proteomics Laboratory (LABPROT), Institute of Chemistry, Federal University
527 of Rio de Janeiro (UFRJ) for technical support in the proteome analysis.

528

529 **Author Contributions**

530

531 **Conceptualization:** Adriana Gonela, Isaac Romani, Gilberto Barbosa Domont, Fábio
532 César Sousa Noqueira.

533 **Data curation:** Talita Mayara de Campos Jumes Gemelli, Isaac Romani, Natália Ferreira
534 dos Santos.

535 **Formal analysis:** Talita Mayara de Campos Jumes Gemelli, Isaac Romani, Natália
536 Ferreira dos Santos, Gilberto Barbosa Domont, Fábio César Sousa Noqueira.

537 **Funding Acquisition:** Adriana Gonela, Gilberto Barbosa Domont, Fábio César Sousa
538 Noqueira.

539 **Investigation:** Talita Mayara de Campos Jumes Gemelli, Isaac Romani, Natália Ferreira
540 dos Santos.

541 **Methodology:** Adriana Gonela, Carlos Alberto Scapim, Gilberto Barbosa Domont, Fábio
542 César Sousa Noqueira, Talita Mayara de Campos Jumes Gemelli, Isaac Romani, Natália
543 Ferreira dos Santos.

544 **Project administration:** Adriana Gonela, Gilberto Barbosa Domont, Fábio César Sousa
545 Noqueira, Talita Mayara de Campos Jumes Gemelli, Isaac Romani, Natália Ferreira dos
546 Santos.

547 **Resources:** Adriana Gonela, Carlos Alberto Scapim, Talita Mayara de Campos Jumes
548 Gemelli, Isaac Romani, Natália Ferreira dos Santos.

549 **Software:** Talita Mayara de Campos Jumes Gemelli, Isaac Romani, Natália Ferreira dos
550 Santos.

551 **Supervision:** Adriana Gonela, Gilberto Barbosa Domont, Fábio César Sousa Noqueira,
552 Maria de Fátima P.S. Machado.

553 **Validation:** Adriana Gonela, Carlos Alberto Scapim, Gilberto Barbosa Domont, Fábio
554 César Sousa Noqueira, Maria de Fátima P.S. Machado.

555 **Visualization:** Adriana Gonela, Carlos Alberto Scapim, Gilberto Barbosa Domont, Fábio
556 César Sousa Noqueira, Maria de Fátima P.S. Machado, Talita Mayara de Campos Jumes
557 Gemelli, Isaac Romani, Natália Ferreira dos Santos.

558 **Writing – original draft, Writing – review & editing:** Adriana Gonela, Talita Mayara
559 de Campos Jumes Gemelli, Isaac Romani, Natália Ferreira dos Santos.

560

561 **References**

562

563 1. Sweley JC, Rose DJ, Jackson DS. Quality traits and popping performance
564 considerations for popcorn (*Zea mays* Everta). Food Reviews International. 2013;
565 29(2):157-177.

566 2. Mishra G, Joshib DC, Pandaa BK. Popping and puffing of cereal grains: a review.

567 Journal of Grain Processing and Storage. 2014; 1(2):34-46.

568 3. Park D, Maga JA. Effects of storage temperature and kernel physical condition on

569 popping qualities of popcorn hybrids. Cereal Chemistry. 2000; 79(4):572-575.

570 4. Ziegler KE. Popcorn. In: Halluer AR, editor. Specialty corns. CRC press: USA; 2001.

571 p. 199-234.

572 5. Borras F, Seetharaman K, Yao N, Robute JL, Percibaldi NM, Eyherabide GH.

573 Relationship between popcorn composition and expansion volume and discrimination

574 of corn types by using zein properties. Cereal Chemistry. 2006; 83(1):86-92.

575 6. Silva WJ, Vidal BC, Pereira AC, Zerbeto M, Vargas H. What makes popcorn pop.

576 Nature. 1993; 362: 417-417.

577 7. Hoseney RC, Zeleznak K, Abdelrahman A. Mechanism of popcorn popping. Journal

578 of Cereal Science. 1983; 1(1):43-52.

579 8. Scheller HV, Ulvskov P. Hemicelluloses. Annual Review of Plant Biology. 2010;

580 61:263-289.

581 9. Carpita NC, Gibeaut DM. Structural models of primary cell walls in flowering plants:

582 consistency of molecular structure with the physical properties of the cell wall during

583 growth. The Plant Journal. 1993; 3(1):1-30.

584 10. Yokoyama R, Rose JKC, Nishitani K. A surprising diversity and abundance of

585 xyloglucan endotransglucosylase/hydrolases in rice: classification and expression

586 analysis. Plant Physiology. 2004; 134(3):1088-1099.

587 11. Eklöf JM, Brumer H. The XTH gene family: an update on enzyme structure, function,

588 and phylogeny in xyloglucan remodeling. Plant Physiology. 2010; 153(2):456-66.

589 12. Moreira-Vilar FC, Siqueira-Soares RC, Finger-Teixeira A, Oliveira DM, Ferro AP,

590 Rocha GJ, et al. The acetyl bromide method is faster, simpler and presents better

591 recovery of lignin in different herbaceous tissues than Klason and thioglycolic acid
592 methods. PLoS One. 2014; 9, e110000.

593 13. Ithal N, Recknor J, Nettleton D, Maier T, Baum TJ, Mitchum MG. Developmental
594 transcript profiling of cyst nematode feeding cells in soybean roots. Mol Plant
595 Microbe Interact. 2007; 20, 510–525.

596 14. Shigeto J, Tsutsumi Y. Diverse functions and reactions of class III peroxidases. New
597 Phytologist. 2016; 209: 1395–1402. doi: 10.1111/nph.13738.

598 15. Laitinen T, Morreel K, Delhomme N, Gauthier A, Schiffthaler B, Nickolov K, et al.
599 A key role for apoplastic H₂O₂ in Norway spruce phenolic metabolism. Plant Physiol.
600 2017; 174:1449-1475.

601 16. Dixon RA, Barros J. Lignin biosynthesis: old roads revisited and new roads explored.
602 Open Biol. 2019; 9: 190215. <http://dx.doi.org/10.1098/rsob.190215>.

603 17. Tobimatsu Y, Schuetz M. Lignin polymerization: how do plants manage the
604 chemistry so well? Current Opinion in Biotechnology. 2019; 56:75–81.

605 18. Damasceno Junior C, Godoy S, Gonela A, Scapim CA, Grandis G, Santos WD, et al.
606 Biochemical composition of the pericarp cell wall of popcorn inbred lines with
607 different popping expansion. Current Research in Food Science. 2022; 5:102–106.

608 19. Robbins ML, Roy A, Wang PH, Gaffoor I, Sekhon RS, de Buanafina MM.
609 Comparative proteomics analysis by DIGE and iTRAQ provides insight into the
610 regulation of phenylpropanoids in maize. Journal of Proteomics. 2013; 93:254-275.

611 20. Thingholm TE, Palmisano G, Kjeldsen F, Larsen MR. Undesirable charge-
612 enhancement of isobaric tagged phosphopeptides leads to reduced identification
613 efficiency. J Proteome Res. 2010; 9:4045-52.

614 21. Nogueira FCS, Palmisano G, Schwämmle V, Campos FAP, Larsen MR, Domont GB,
615 et al. Performance of isobaric and isotopic labeling in quantitative plant proteomics.
616 J Proteome Res. 2012; 11:3046-52.

617 22. Santos MDM, Lima DB, Fischer JSG, Clasen MA, Kurt LU, Camillo-Andrade AC,
618 et al. Simple, efficient and thorough shotgun proteomic analysis with PatternLab V.
619 Nature protocols. 2022. <https://doi.org/10.1038/s41596-022-00690-x>

620 23. Kanehisa M, Goto S, Sato Y, Furumichi M, Tanabe M. KEGG for integration and
621 interpretation of large-scale molecular data sets. Nucleic Acids Research. 2015;
622 10(1):109-114.

623 24. Tian T, Liu Y, Yan H, You Q, Yi X, Du Z, et al. AgriGO v. 2.0: a GO analysis toolkit
624 for the agricultural Community. Nucleic Acids Res. 2017; 45:W122-W129.

625 25. Richardson DL. Pericarp thickness in popcorn. Agronomy Journal. 1960; 52(2):77-
626 80.

627 26. Mohamed AA, Ashman RB, Kirleis AW. Pericarp thickness and other kernel physical
628 characteristics relate to microwave popping quality of popcorn. Journal of Food
629 Science. 1993; 58 (2):342-346.

630 27. Ho LC, Kannenberg LW, Hunter RB. Inheritance of pericarp thickness in short season
631 maize inbreds. Canadian Journal of Genetics and Cytology. 1975; 17(4):621-629.

632 28. Tandjung AS, Janaswamy S, Chandrasekaran R, Aboubacar A, Hamaker BR. Role of
633 the pericarp cellulose matrix as a moisture barrier in microwaveable popcorn.
634 Biomacromolecules. 2005; 6(3):1654-1660.

635 29. Dong Y, Wang Q, Zhang L, Du C, Xiong W, Chen X, et al. Dynamic proteomic
636 characteristics and network integration revealing key proteins for two kernel tissue
637 developments in popcorn. PLoS One. 2015; 10(11):77-86.

638 30. Sampedro J, Cosgrove DJ. The expansin superfamily. **Genome Biology**. 2005; 6:242.

639 doi:10.1186/gb-2005-6-12-242.

640 31. Carpita NC, Ralph J, McCann MC. The cell wall. In: Buchanan BB, Gruissem W,

641 Jone RL, editors. *Biochemistry & Molecular Biology of Plants*. Oxford: John Wiley

642 & Sons, Ltd.; 2015. p. 45-110.

643 32. García-Lara S, Bergvinson DJ, Burt AJ, Ramputh AI, Díaz-Pontones DM, Arnason

644 JT. The role of pericarp cell wall components in maize weevil resistance. *Crop*

645 *Science*. 2004; 44:1546-1552.

646 33. Ito GM, Brewbaker JL. Genetic analysis of pericarp thickness in progenies of eight

647 corn hybrids. *J Amer Soc Hort Sci*. 1991; 116(6):1072-1077.

648 34. Wu X, Wang B, Xie F, Zhang L, Gong J, Zhu W, et al. QTL mapping and

649 transcriptome analysis identify candidate genes regulating pericarp thickness in sweet

650 corn. *BMC Plant Biology*. 2020; 20:117. doi.org/10.1186/s12870-020-2295-8.

651 35. Kaur S, Rakshit S, Choudhary M, Das AK, Kumar RR. Meta-analysis of QTLs

652 associated with popping traits in maize (*Zea mays* L.). *PLoS One*. 2021; 16(8):

653 e0256389. <https://doi.org/10.1371/journal.pone.0256389>.

654 36. Randolph LF. Developmental morphology of the caryopsis in maize. *J Agr Res*. 1936;

655 53:881-916.

656 37. Rose JK, Braam J, Fry SC, Nishitani K. The XTH family of enzymes involved in

657 xyloglucan endotransglucosylation and endohydrolysis: current perspectives and a

658 new unifying nomenclature. *Plant Cell Physiology*. 2002; 43(12):1421-1435.

659 38. Hara Y, Yokoyama R, Osakabe K, Toki S, Nishitani K. Function of xyloglucan

660 endotransglucosylase/hydrolases in rice. *Annals of Botany*. 2014; 114(6):1309–1318.

661 39. Sharples SC, Nguyen-Phan TC, Fry SC. Xyloglucan endotransglucosylase/hydrolases

662 (XTHs) are inactivated by binding to glass and cellulosic surfaces, and released in

663 active form by a heat-stable polymer from cauliflower florets. *Journal of Plant*
664 *Physiology*. 2017; 218:135-143.

665 40. Fu, MM, Liu C, Wu F. Genome-wide identification, characterization and expression
666 analysis of xyloglucan endotransglucosylase/hydrolase genes family in barley
667 (*Hordeum vulgare*). *Molecules*. 2019; 24:1935-1946.

668 41. Fry SC, Smith RC, Renwick KF, Martin DJ, Hodge SK, Matthews, KJ. Xyloglucan
669 endotransglycosylase, a new wall-loosening enzyme activity from plants.
670 *Biochemical Journal*. 1992; 282(pt 3):821–828.

671 42. Fanutti C, Gidley MJ, Reid JS. Action of a pure xyloglucan endo-transglycosylase
672 (formerly called xyloglucan-specific endo-(1→4)-beta-D-glucanase) from the
673 cotyledons of germinated nasturtium seeds. *The Plant Journal*. 1993; 3(5):691-700.

674 43. Yokoyama R, Nishitani K. A comprehensive expression analysis of all members of a
675 gene family encoding cell-wall enzymes allowed us to predict cis-regulatory regions
676 involved in cell-wall construction in specific organs of *Arabidopsis*. *Plant Cell*
677 *Physiology*. 2001; 42(10):1025-1033.

678 44. Saladié M, Rose JK, Cosgrove DJ, Catalá C. Characterization of a new xyloglucan
679 endotransglucosylase/hydrolase (XTH) from ripening tomato fruit and implications
680 for the diverse modes of enzymatic action. *Plant Journal*. 2006; 47(2): 282-295.

681 45. Liu Y, Liu D, Zhang H, Gao H, Guo X, Wang D, et al. The α - and β -expansin and
682 xyloglucan endotransglucosylase/hydrolase gene families of wheat: Molecular
683 cloning, gene expression, and EST data mining. *Genomics*. 2007; 90(4):516–529.

684 46. Uozu S, Tanaka-Ueguchi M, Kitano H, Hattori K, Matsuoka M. Characterization of
685 XET related genes in rice. *Plant Physiology*. 2000; 122(3): 853-859.

686 47. Saab IN, Sachs MM. A flooding-induced xyloglucan endo-transglycosylase homolog
687 in maize is responsive to ethylene and associated with aerenchyma. *Plant Physiology*.
688 1996; 112(1): 385-391.

689 48. NCBI. LOC542059 xyloglucan endo-transglycosylase/hydrolase [*Zea mays*].

690 Available from:

691 <https://www.ncbi.nlm.nih.gov/gene?Db=gene&Cmd=DetailsSearch&Term=542059>.

692 49. Iurlaro A, Caroli MD, Sabella E, Pascali MD, Rampino P, Bellis LD, et al. Drought
693 and heat differentially affect XTH expression and XET activity and action in 3-day-
694 old seedlings of durum wheat cultivars with different stress susceptibility. *Frontiers
695 in Plant Science*. 2016; 7:10-26.

696

697

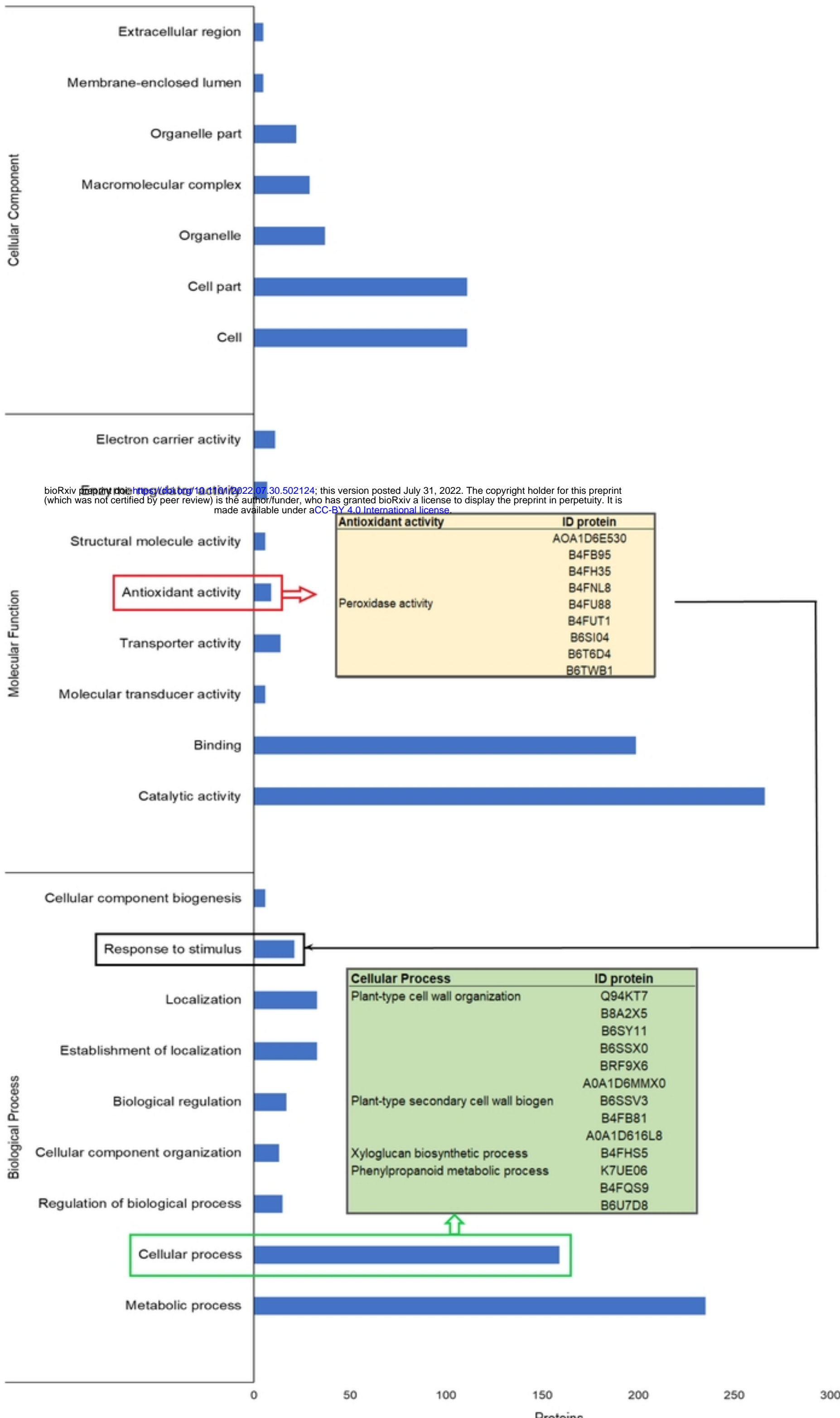
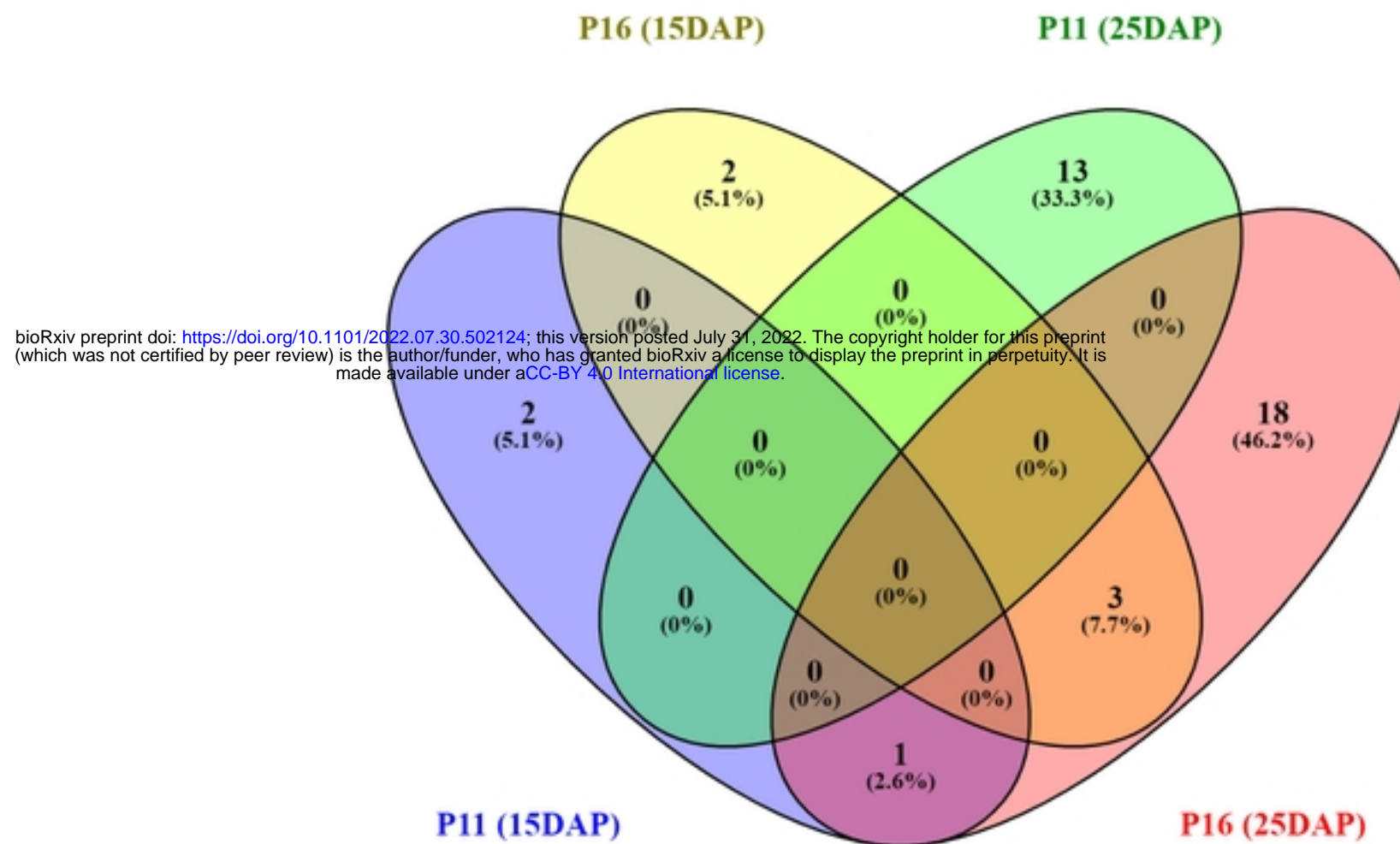


Fig 1

(A)



(B)

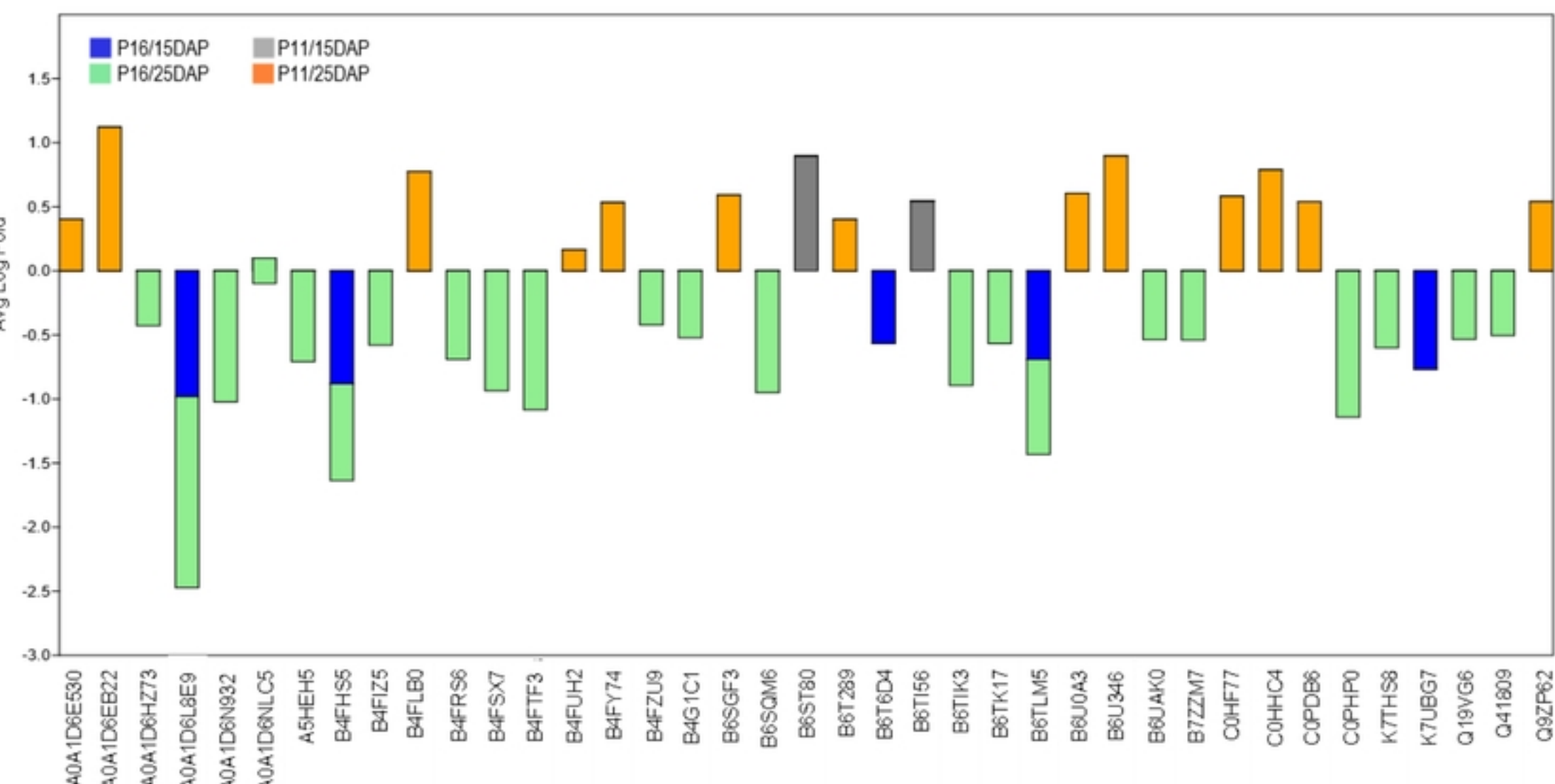


Fig 2



Fig 3